Optimum Stiffness Values for Impact Element Models to Determine Pounding Forces between Adjacent Buildings

Yazan Jaradat, Harry Far*

School of Civil and Environmental Engineering, Faculty of Engineering and Information Technology, University of Technology Sydney (UTS), Australia

(Received , Revised , Accepted)

Abstract

Structural failure due to seismic pounding between two adjacent buildings is one of the major concerns in the context of structural damage. Pounding between adjacent structures is a commonly observed phenomenon during major earthquakes. When modelling the structural response, stiffness of impact spring elements is considered to be one of the most important parameters when the impact force during collision of adjacent buildings is calculated. Determining valid and realistic stiffness values is essential in numerical simulations of pounding forces between adjacent buildings in order to achieve reasonable results. Several impact model stiffness values have been presented by various researchers to simulate pounding forces between adjacent structures. These values were mathematically calculated or estimated. In this study, a linear spring impact element model is used to simulate the pounding forces between two adjacent structures. An experimental model reported in literature was adopted to investigate the effect of different impact element stiffness k on the force intensity and number of impacts simulated by Finite Element (FE) analysis. Several numerical analyses have been conducted using SAP2000 and the collected results were used for further mathematical evaluations. The results of this study concluded the major factors that may actualise the stiffness value for impact element models. The number of impacts and the maximum impact force were found to be the core concept for finding the optimal range of stiffness values. For the experimental model investigated, the range of optimal stiffness values has also been presented and discussed.

Keywords: *Stiffness of Impact Spring; Pounding Forces; k Value; SAP2000; Linear Spring Impact Model*

Introduction

Structural pounding refers to the lateral collisions between adjacent buildings during earthquakes. It occurs when adjacent buildings vibrate out of phase and the at-rest separation is insufficient to accommodate their relative motions (Maison & Kasai 1992; Tabatabaiefar & Clifton 2016, Far et al. 2019). It is a complex phenomenon involving plastic deformations at contact points, local cracking or crushing, fracturing due to impact, friction and so on (Jankowski 2008).

As stated by several researchers Anagnostopoulos (1988), Jankowski & Mahmoud (2016), Rahman et al. (2000) and Naserkhaki et al. (2012) the main reason for seismic pounding is insufficient separation between adjacent buildings. Differences in the adjacent buildings' natural periods (free vibration), mass and/or stiffness values have been identified to be the most important reasons for seismic pounding between adjacent buildings to take place. The mentioned reasons have direct impact on structure out-of-phase vibration during an

* Corresponding author: Senior Lecturer in Structural Engineering, School of Civil and Environmental Engineering, Faculty of Engineering and Information Technology, University of Technology Sydney (UTS), Building 11, Level 11, Broadway, Ultimo NSW 2007 (PO Box 123), Email: harry.far@uts.edu.au

earthquake, may cause architectural and structural damage, and sometimes may lead to whole structure collapse (Sheikh et al. 2012; Tabatabaiefar et al. 2012; Fatahi & Tabatabaiefar 2014, Rahimi and Soltani 2017)

Two analytical techniques are available for simulating pounding between two adjacent structures, namely, the contact element method and the stereo-mechanical approach. In the contact element model, a contact element is activated when the adjacent structures come into contact. A spring with high stiffness is used to avoid overlapping between adjacent segments, sometimes in conjunction with a damper. The contact elements used in the past include;

- The linear spring model Filiatrault et al. (1995) and Maison & Kasai (1992);
- Kelvin–Voigt element model or linear viscoelastic model Anagnostopoulos & Spiliopoulos (1992), Polycarpou & Komodromos (2010), Mate et al. (2012), Crozet et al. (2017) and López-Almansa & Kharazian (2018);
- Hertz model or nonlinear elastic model Chau et al. (2003), Abdel Raheem (2006) and Mate et al. (2012);
- Hertz-damp model or Hertz model with nonlinear damper Muthukumar & Desroches (2004) and Mate et al. (2012); and
- The nonlinear viscoelastic model Jankowski (2006), Jankowski (2008), Mahmoud & Jankowski (2009), Mahmoud & Jankowski (2011) and Naderpour et al. (2016).

The contact element approach has its limitations, with the exact value of spring stiffness to be used being unclear. Moreover, using a spring of very high stiffness can result in unrealistically high impact forces and also lead to numerical convergence problems. The stereo-mechanical approach, applies the classical theory of impact, assumes instantaneous impact and uses momentum balance and the coefficient of restitution to modify velocities of the colliding bodies after the impact. When precise pounding is required, it is not recommended to use this approach, since it is not a force-based concept Jankowski (2005) and Mate et al. (2012). Moreover, the stereo-mechanical method is not commonly used in pounding analyses, and as a result, it cannot be considered suitable for finite element simulation (Muthukumar & Desroches 2004). The stereo-mechanical approach and contact element models predict similar displacement responses. However, the contact element models predict higher accelerations due to pounding, while the system acceleration responses from the stereo-mechanical approach are smaller than those from the contact models, (Muthukumar & Desroches 2004). Researchers often simulate seismic pounding numerically. This is essential to demonstrate a structure's response, with a lower cost, faster results and larger variety of models. However, for structural pounding analysis, the primary issue for utilising contact element models is to determine the parameters of the impact models, especially the stiffness of impact element model k. The k parameter is used for the numerical simulation to compare between numerical and physical experiments (Guo et al. 2012). To calculate the stiffness of impact element model k, several researchers have proposed different methods and equations. Some studies (e.g. Wada 1984; Anagnostopoulos 1988; Masion 1992) used steel and concrete models to determine the stiffness of the impact model. Some other studies (Maison & Kasai 1992; Jankowski 2005; Cole et al. 2012) proposed some random and calculated values for k. In this this study, a parametric analysis was performed to investigate the effect of different values of impact element model stiffness k on the force intensity and number of impacts simulated by FE analysis. The main objective of the current paper is finding the optimum stiffness values for impact element models. This is essential to perform an accurate dynamic analysis in order to determine seismic pounding forces between adjacent buildings.

Previous Work to Calculate the Stiffness of Impact Element Model

Stiffness of impact spring element is considered to be one of the most important parameters when the impact force during collision is calculated. Unfortunately, there is no accepted method of determining its value (Khatiwada & Chouw 2014). The only analytical formula for k was derived by Hertz's law Lankarani & Nikravesh (1992) and used by Abdel Raheem (2006) and Chau et al. (2003) Many studies have been carried out suggesting various assumptions for assigning stiffness to the spring element, which are described in this section.

Wada et al (1984) integrated a gap element with stiffness equal to the axial stiffness of the beams and slab at the impact level as follows:.

$$k = K_b + K_s = \frac{EA_b}{L_b} + \frac{EA_s}{L_s} \quad (1)$$

where A_b is the cross-sectional area of the beam, A_s is the cross sectional area of the slab, E is the modulus of elasticity, and L is the length of the element in the direction perpendicular to the contact surfaces.

Anagnostopoulos (1988) suggested a gap element with stiffness twenty times larger than the lateral stiffness of the rigid SDOF system as follows:

$$k = \frac{Lateral\ Load}{Displacement} \times 20 \quad (2)$$

Masion and Kasai (1992) proposed a spring stiffness equivalent to the axial stiffness of a floor slab having the width of the adjacent building at the impact level.

$$k = \frac{EA_s}{L} \quad (3)$$

Cole et al. (2012) adopted a spring element with stiffness equal to the smaller axial stiffness of the colliding floor at point of contact. These stiffness's were calculated by taking tributary width measurements when beams were aligned. The parallel beam aligned to the direction of the anticipated contact force is considered in calculation, while the perpendicular beam is ignored. Their stiffness was added to that calculated in the diaphragm.

$$K_i = EA_i/L \quad \text{and} \quad A_i = w_i t \quad (4)$$

$$k = K_s + K_b = \frac{EA_s}{L} + \frac{EA_b}{L} \quad (5)$$

where E, t and w_i are the modulus of elasticity, slab thickness and average element width respectively.

Based on an experimental study carried out by Jankowski (2005) and Van et al. (1991), the impact stiffness parameter value for concrete to concrete was $\beta = 2.75 \times 10^9 N/\text{m}^{3/2}$ and $k = 93.5$ KN/mm for the nonlinear viscoelastic model and linear viscoelastic model, respectively; values for steel to steel impact were $\beta = 9.9 \times 10^{10} N/\text{m}^{3/2}$ and $k = 1400\ kN/\text{mm}$ for the nonlinear viscoelastic model and linear viscoelastic model, respectively.

Adopted Methodology

The purpose of the present study is to compare various methods of calculating the stiffness of impact element model k in order to manifest the optimal method of calculating this parameter. The previous section briefly addressed some of these methods, which showed that researchers have proposed them by using theoretical calculations. Moreover, other researchers have also reused these theoretical studies without verifying the accuracy of these methods. This highlights the need for reversing the techniques of finding the most appropriate method for calculating the stiffness of impact element parameter. A revised method has been proposed by analysing a shake table experiment to conclude the stiffness of impact element model parameter. Thus, a previous experiment carried out by Filiatrault et al. (1995) was modelled. The experiment presented the results of shake table tests of pounding between adjacent three- and eight-storey single-bay steel framed model structures. All data were abstracted from the experiment chart diagrams. Then, the data were processed by SAP2000 v20 program. This program simulates shake table relative displacement and pounding impact forces. The simulation outputs were then compared with Filiatrault's et al. (1995) experiment results, which showed a good agreement. The stiffness of impact element model *k* was derived from Filiatrault's et al. (1995) experiment. Finding this parameter from shake table tests is more accurate than implementing theoretical equations. The numerical results have shown good agreement with Filiatrault's et al. (1995) experiment.

It should be noted that unlike past studies in which the proposed stiffness values were directly derived from numerical analysis, in this study reverse engineering method was adopted to extract the values from an experimental model. Then the obtained parameters have been used in numerical analyses. It is a method of validating the numerical model by using experimental data.

Numerical Investigation

As described in the previous section, some graphical diagrams were initially prepared for abstracting parameters from the plotted points. Technically this is possible by deploying a Java program, known as plotdigitzer, coded by (Huwaldt & Steinhorst 2015). The program scans the diagram in image format and reads the manually assigned points. The original diagram looks like a vibrant line with low resolution dots. This low resolution was one of the drawbacks in achieving accurate digital values.

After abstracting variables, a diagram was plotted by using the abstracted numbers to deliberately verify the similarity between the original diagram and the plotted diagram. Moreover, the abstracted variables were exported to SAP2000. It is essential to replicate the shake table experiment by using numerical simulation. For this reason, a similar case was designed to the previously mentioned experiment. The aim of this step is to mimic the adjacent building displacement and pounding force with the shake table outcome. Numerical results showed a very good accuracy in comparison with the shake table experiment. The shake table experiment was conducted with a 15 mm gap and 0 mm gap; then, similarly, a 15 mm gap and 2 mm gap were applied. Fig. 1 compares the test experimental results and the replicated SAP2000 demonstration.

To model the gap between the adjacent buildings, a nonlinear gap element was used. Material, masses, dimensions and all elements were defined similar to the actual values of experimental frame models.

Preliminary System Identification Tests

The software used for numerical investigation as a three-dimensional frame is known as SAP2000 version 20 (SAP 2000). This software is appropriate to output time-history analysis with a nonlinear gap element, and specifically, to model pounding conditions. Ritz vector was selected as the mode type, in the modal load case according to Noman et al. (2016). The selected maximum numbers of modes were 99 and 99% target dynamic participation ratios; these are used for acceleration and link element. To numerically model the flexibility in SAP2000 that occurred at the beam-column connections, end length offsets were used. The flexibility at the joints where a beam connected to a column can significantly impact the overall behaviour of a frame structure. This is essential to correctly model the structure. The flexibility of the beam-column joints were modelled using a rigid end offsets approach, where a rigid link connects the end of the beam at the column face to the column centre line. All the frames model were selected, then assigned frame end length offsets. A rigid zone factor equal to 1 was defined, which means the connection is fully rigid. The natural periods for both experimental and numerical models show very good agreement, with a very low mean square error rate as illustrated in Table 1.

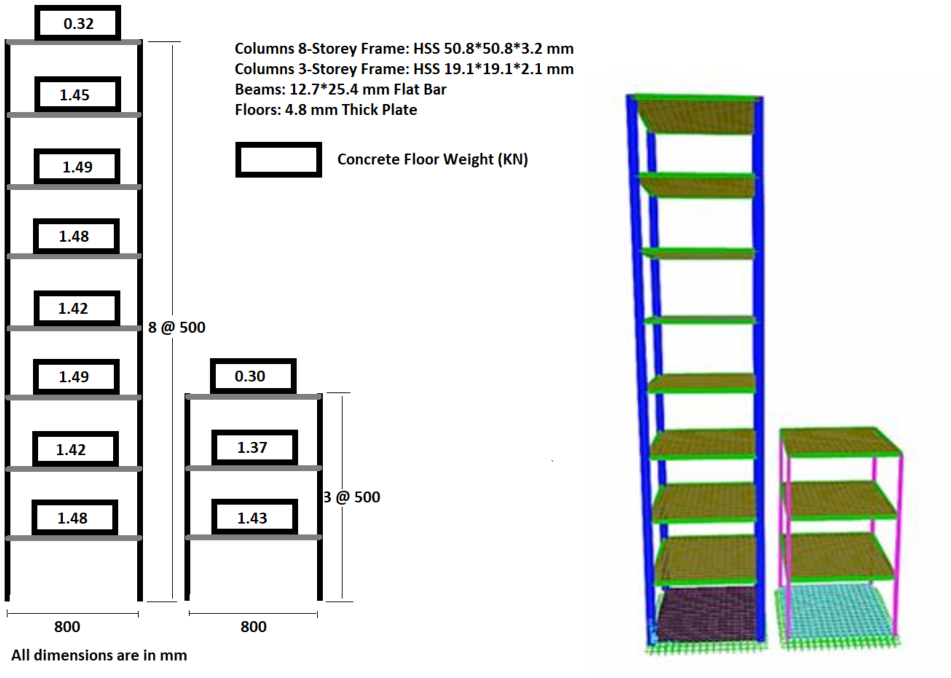

(a) **(b)**

Fig. 1 a) Experimental frame Filiatrault et al. (1995); b) Three-dimensional SAP2000 model

Table 1 Natural periods for both experimental and numerical models

	Experimental		**Numerical**
	Free Vibration Test		
	Mode1		**Mode1**
Structural Configuration	Period (sec)	Damping (%)	Period (sec)
3-Storey No-Pounding	0.341	1.00	0.33394
8-storey No-Pounding	0.605	1.50	0.59825
3-Storey/8-Storey Pounding	0.567	1.60	0.55441

Nonlinear dynamic analysis or Fast Nonlinear Analysis (FNA) with 5000 time steps at 0.002 second step size was carried out in SAP2000. The dynamic load applied to the model was El-Centro earthquake time-history acceleration record with Peak Ground Acceleration (PGA) of 0.15 g. There has been uncertainty surrounding selection of the most reliable method of analysis. Two popular methods are known by researchers are FNA and direct integration, by Newmark (1959). The second method implements the standard parameters $\beta = \frac{1}{4}$ and $\lambda = \frac{1}{2}$. In order to determine the most appropriate method, a pilot test was conducted using both methods, Newmark and FNA based on Huang & Syu (2014). The test was conducted for top floor relative displacement time-histories for the no-pounding case. The results showed a very good agreement between the two methods. Therefore, FNA was chosen, since it is a time saver in analysis, unlike Newmark, which consumes time dramatically.

Impact Link Element

Filiatrault et al. (1995) experimentally used three special impact elements to measure impact force time-histories between the first three levels of adjacent buildings. To determine the element axial stiffness employed in the numerical studies, they performed compressive static tests on each impact device. Based on these tests, an element axial stiffness of 12.8 kN/mm was used in the numerical studies.

In the numerical model, the adjacent three-storey frame is connected to the eight-storey frame using a link gap element at each level; these parameters are available in SAP2000 (SAP 2000). A gap link element model, also known as a linear spring model, and the contact force-displacement relationship are shown in Fig. 2.

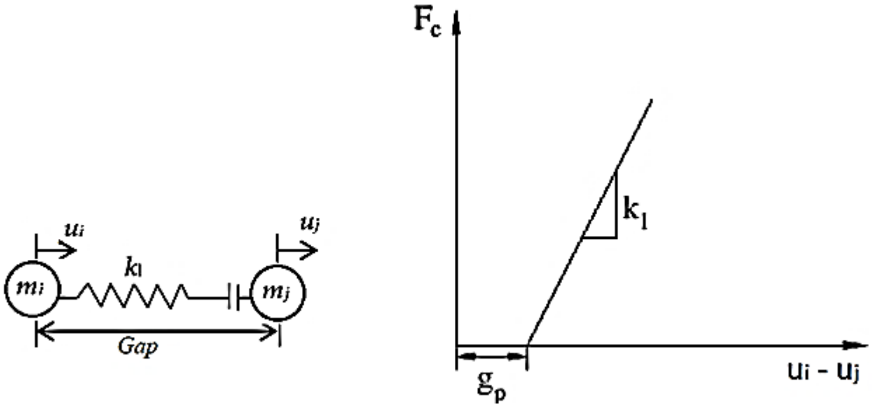

Fig. 2 Linear spring model and contact force relationship

Comparison between Numerical and Experimental Results for No-pounding Condition

This step involves a comparison between the numerical top floor relative displacements and the corresponding experimental time-history displacements under no-pounding condition for the scaled El Centro ground motion (PGA = 0.15 g). This condition imposes a large gap to ensure the frames will not hit each other, as shown in Fig. 3. Small differences in the amplitude and phase exist between the expectations of the numerical model and the experimental results for the top floor of the three-storey building (Figure 3a) with an error rate of 11.57%. On the other hand, the results show very good agreement for the top floor of the eight-storey building (Figure 3b) and the error rate determined to be 20.50%.

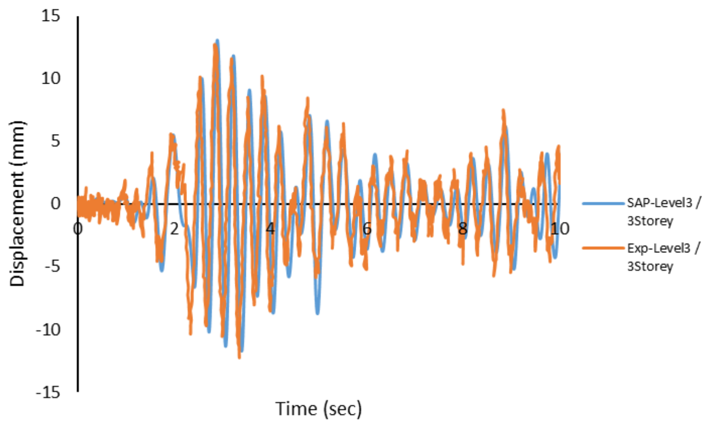

(a)

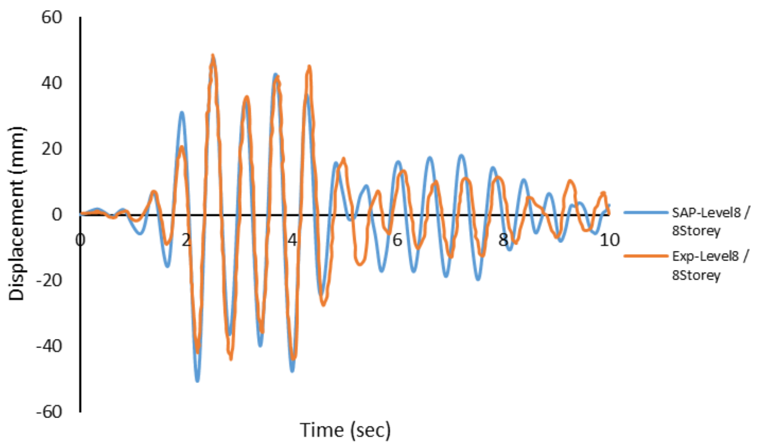

(b)

Fig. 3 Top floor relative displacement time-histories for no-pounding condition; a) 3 storey model; b) 8 storey model

Comparison between Numerical and Experimental Results for Pounding Condition

Relative Displacement Time-histories

Numerical results were compared to their experimental counterparts for relative displacement time-histories at the top of each frame structure under scaled El Centro ground motion, with an initial separation gap of 0.0 mm and 15.0 mm, respectively. Fig. 4 shows the displacement response of the top floor for the three- and eight-storey buildings. The amplitude and phase are very similar in the case of the eight-storey building (Fig. 4b), while there was some dissimilarity in the case of the three-storey building in peak displacement response (Fig. 4a). Fig. 5 compares numerical and experimental relative displacement time-histories at the top floor of three- and eight-storey buildings for 0.0 mm separation gap.

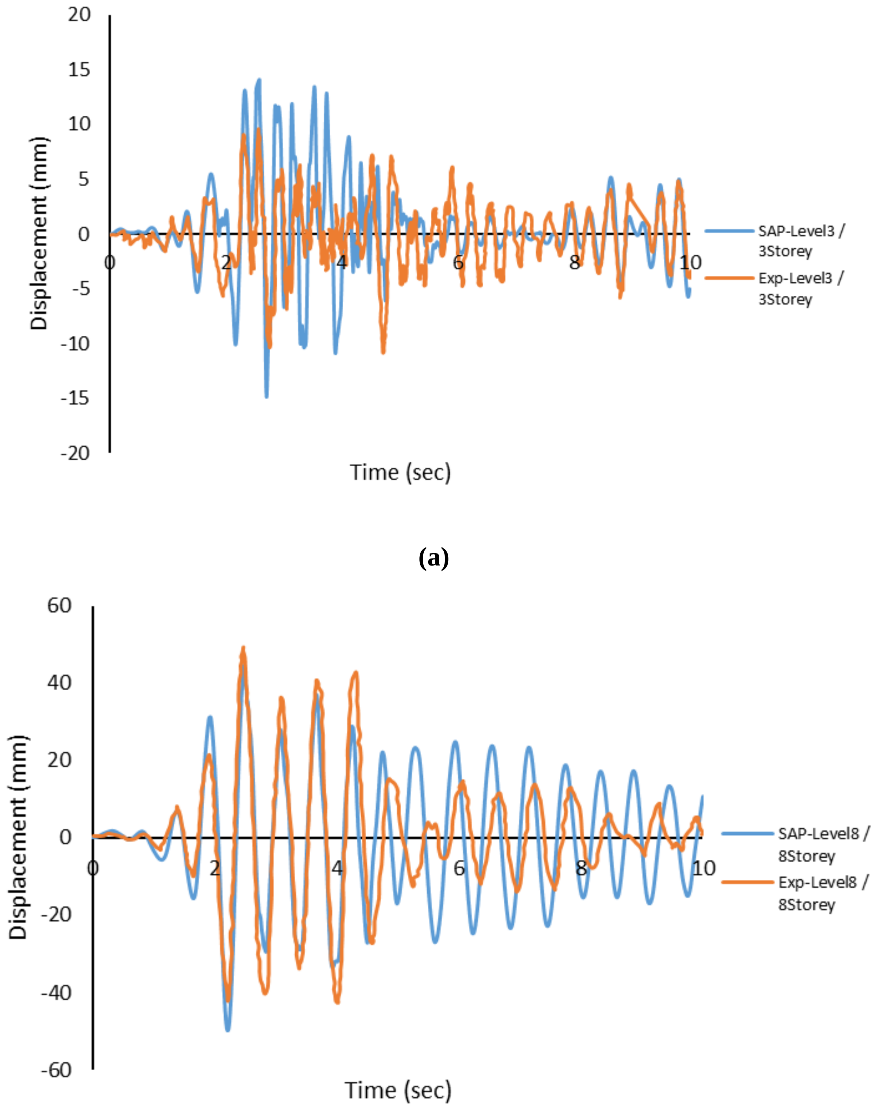

(a)

(b)

Fig. 4 Top floor relative displacement time-histories for pounding between floor diaphragms, experimental vs numerical models with 15.0 mm gap; a) 3 storey model; b) 8 storey model

Impact Force Time-histories

Fig. 6 compares the third floor impact force time-histories between the numerical and experimental models for an initial separation gap of 15.0 mm for the scaled El Centro ground motion (PHA = 0.15 g). Very few impacts occurred within the first five seconds of the response, and the experimental time and amplitudes of the contact forces are well predicted by both models, with slightly higher peaks in the numerical model. No impact was recorded between the first and the second floors for both numerical and experimental models. For 0.0 mm separation gap between the three-storey building and adjacent eight-storey building, Fig. 7 and Fig. 8

show the third and first floor impact time-histories at the same floor levels. It can be seen that the time and amplitudes of the contact forces for the third floor are in good agreement, while the numerical model shows very large peak impact values for the first floor. This was caused by a vulnerability of the impact device during the experiment since the device malfunctioning caused a lack of results for the second floor. It was noticed that in Figures 6 and 8, the peak numerical and experimental impact force results do not match. This mismatch may refer to experimental errors that was mentioned by Filiatrault et al. (1995). Therefore, it is possible that the numerical results are more accurate than the experimental results in some cases.

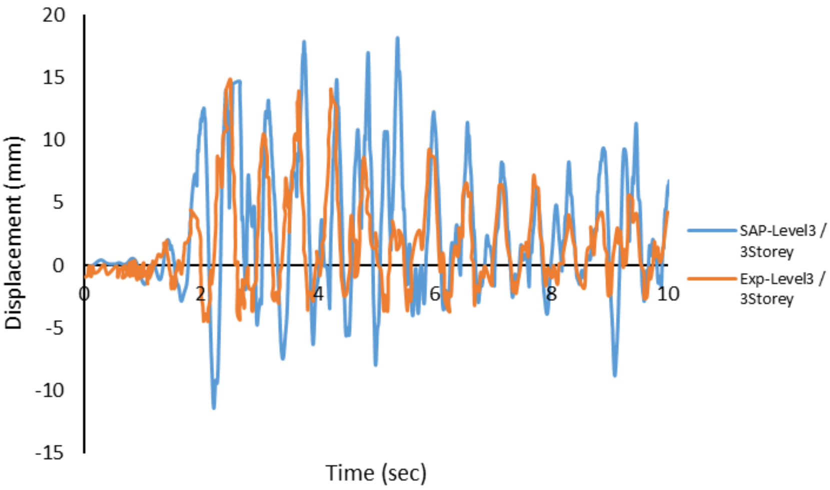

(a)

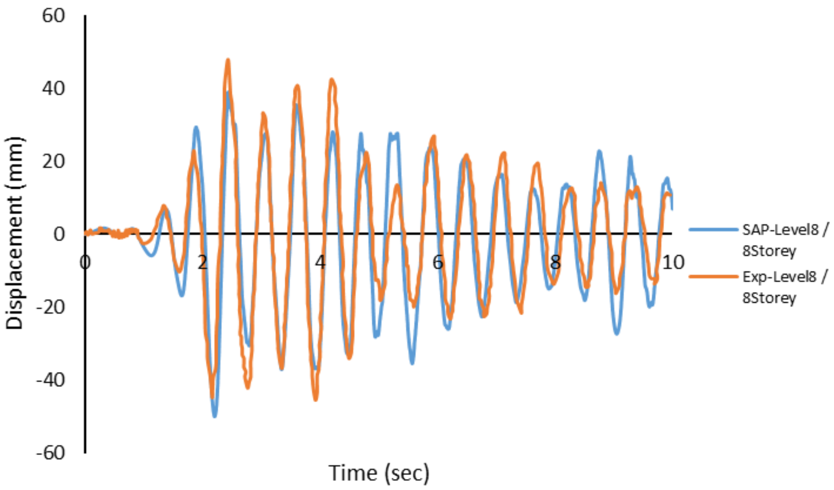

(b)

Fig. 5 Top floor relative displacement time-histories for pounding between floor diaphragms, experimental vs numerical models with 0.0 mm gap; a) 3 storey model; b) 8 storey model

Stiffness of Gap Link Element

As mentioned in the second section of this paper, several researchers have carried out studies suggesting various assumptions for assigning stiffness to the spring element k. These values were calculated based on Filiatrault et al. (1995) experiment as follows:

a) Based on Eq. 1 by Wada et al. (1984), $k = \frac{200000\times 322.58}{800} + \frac{200000\times 60.96}{800} = 95{,}885\ \mathrm{N/mm} = 96\ \mathrm{kN/mm}$

b) Based on Eq. 2 by Anagnostopoulos (1988), $k = \frac{1000}{5.49} = 182.149\ \mathrm{N/mm}\ \times 20\ =\ 4\ \mathrm{kN/mm}$

c) Based on Eq. 3 by Maison & Kasai (1992), $k = \frac{20000\times 3840}{800} = 959{,}000\ \mathrm{N/mm}\ = 959\ \mathrm{kN/mm}$

d) Based on Eq. 4, 5 by Cole et al. (2012), $k = \frac{200000\times 1920}{800} + \frac{200000\times 322.58}{800} = 560{,}645\ \mathrm{N/mm} = 560\ \mathrm{kN/mm}$

e) According to Jankowski (2005) for full scale structure, $k = 1400\ \mathrm{kN/mm}$. Adopted for this experiment, $k = 1400\ \times \frac{1}{8} = 175\ \mathrm{kN/mm}$.

Different k values have been calculated based on the above-mentioned studies. The main purpose is to investigate the major effects of k value variation on displacements and impact forces. It is worth mentioning that the structural period and damping as well as height and mass have not been included in this study since these parameters are independent from k value variation. Figs. 9 and 10 compare different k values for the top floor displacements of the three-storey building model and the impact force at the third floor level, respectively. Comparing the results illustrated in Fig. 9, the computed displacement amplifications due to pounding are not sensitive to changes in the stiffness of the impact elements k value simulating the collisions. Insensitivity of displacement response to spring stiffness has also been reported by Anagnostopoulos (1988), Anagnostopoulos & Spiliopoulos (1992) and Maison & Kasai (1992).

However, as Fig. 10 depicts, k value variation makes noticeable difference in term of time and amplitudes. Two hypotheses can be concluded from the numerical experiments, these are related to the number of impacts and the peak impact force. It was noticed that the number of impacts depends on the k value, unlike the peak force, which showed no relation with the k value. Fig. 10 illustrates these findings, where the number of impact has reverse proportion with k value. For instance, the highest k value has caused only 5 impacts, while the lower k value has caused a higher number of 6 impacts. On the other hand, the peak impact force showed no relation with the k value, for instance, when k = 959 kN/mm the peak force was 23.77 kN, while for k = 560 kN/mm the peak force was 27.95 kN; and for k =175 kN/mm the peak force was 24.96 kN. However, these findings cannot be explained without further experimental investigation and studies are need to approve these hypothesis.

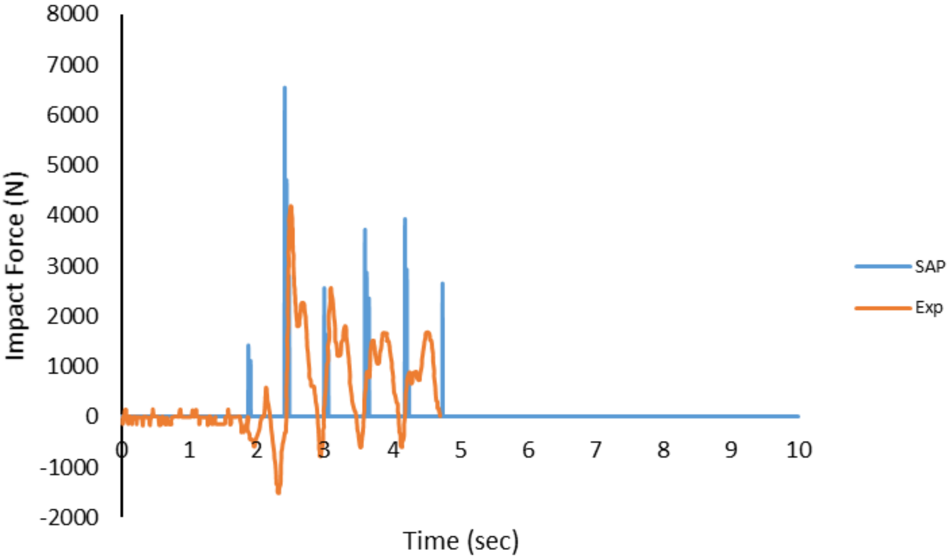

Fig. 6 Third floor impact time-histories for pounding between floor diaphragms, 15.0 mm gap

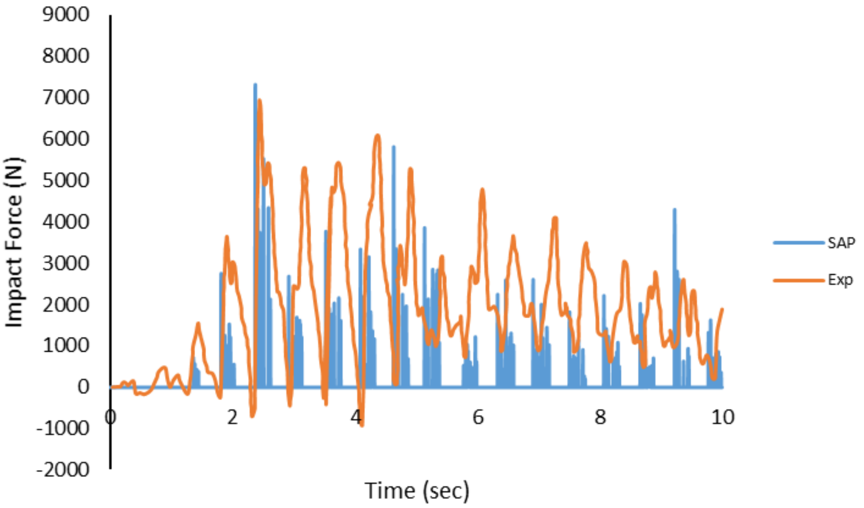

Fig. 7 Third floor impact time-histories for pounding between floor diaphragms, experimental vs numerical models with 0.0 mm gap

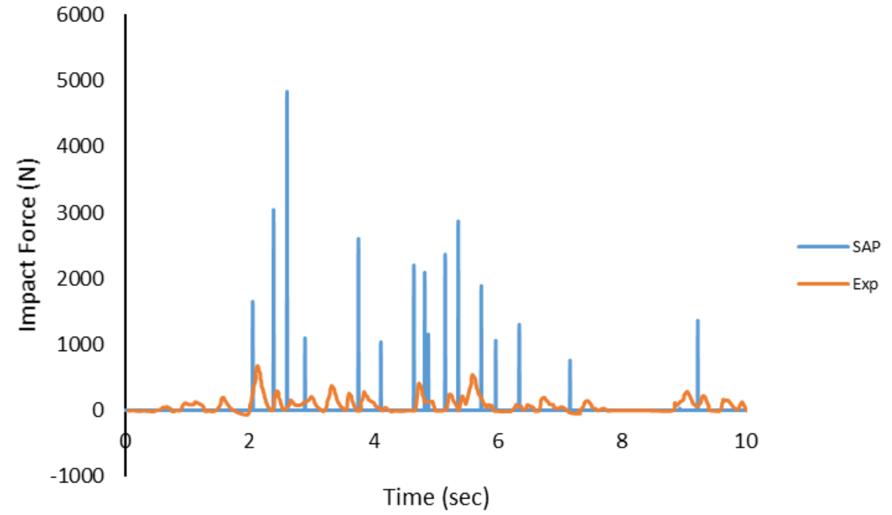

Fig. 8 First floor impact time-histories for pounding between floor diaphragms, experimental vs numerical results with 0.0 mm gap

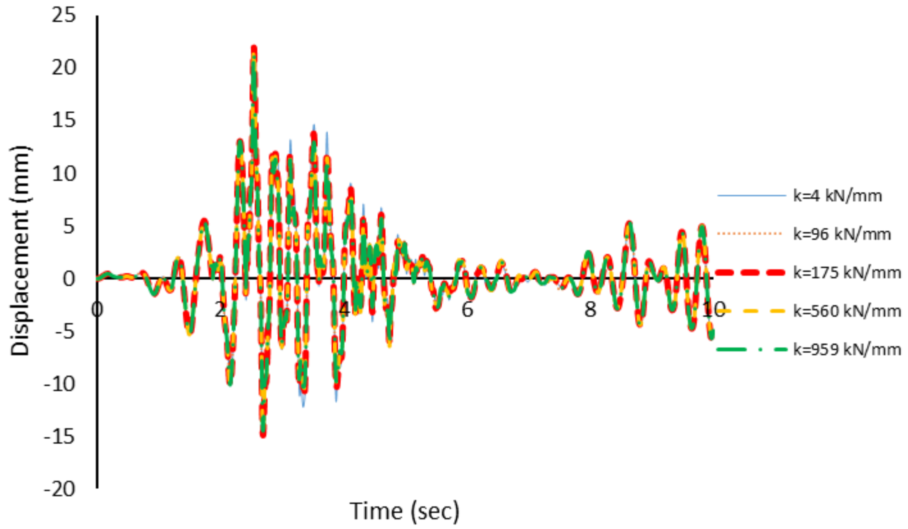

Figure 9: Top floor relative displacement time-histories for three-storey frame with several *k* values, 15.0 mm gap

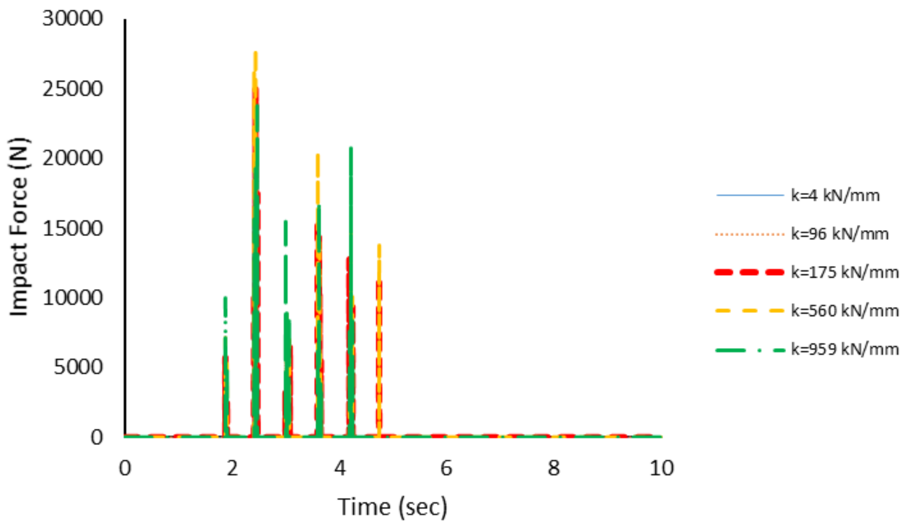

Figure 10: Third floor impact time-histories for pounding between floor diaphragms with several *k* values, 15.0 mm gap

Proposed Stiffness of Gap Link Element *k*

Stiffness of impact spring element is a critical value, and one for which many researchers have suggested a wide range of values. Finding the most appropriate *k* value is one of the major hurdles on conducting numerical simulation. Researchers suggest various methods of assigning the value of *k*, as explained previously in Previous Work to Calculate the Stiffness of Impact Element Model. The test results of several pounding experiments in the literature indicated that actual contact stiffness is significantly smaller than the theoretical values, although the structural response, such as acceleration, displacement and pounding force, can be effectively predicted by using the identified or given stiffness values. For instance, Filiatrault's experiment by Filiatrault et al. (1995), showed a small value of *k*, which manifested some doubts and debates, since this value may not represent reality. This debate leads to further investigations regarding the value of *k*, which can be more appropriate and better accepted by the scientific domain. In summary, the investigation results of this study suggest an approximate value of *k*.

A wide range of *k* values were chosen in this investigation, spanning from 4 to 1300 kN/mm, including the ones suggested by the abovementioned scholars. Considering this wide range of values was essential to formulate a method for choosing the medium value. The same numerical simulation was conducted several times with a different value of *k* each time.

The suggested *k* value has been confirmed and validated by numerical simulation. Twenty numerical analysis were conducted using SAP2000 software, and the resulted values were collected for further mathematical evaluation. Three different parameters were defined in this study including the number of impacts between the adjacent buildings, the maximum impact force and the total impact force. It's worth mentioning that mathematical calculations were suggested from the major impacts on building damage patterns according to Kasai & Maison (1997) and Jeng & Tzeng (2000). This suggestion was the main pillar of calculating the *k* value in this study. Generally, pounding can be effective if the impact force is high and the number of impacts are large. However, as per numerical analysis, the impact forces are not force equivalent, since some impacts have higher momentum than others.

After reviewing all numerical analyses, it was found that the total impact force replicates the total number of impacts, in another words, the total impact force depends on the number of impacts. This intuitively indicates that the total impact force can be ignored. Therefore, two major factors should be further investigated in the numerical analysis, these are the total number of impact and the maximum impact force.

Figs. 11 to 14 illustrate the relationship between the number of impacts and the maximum impact force using several *k* values for 2 mm, 15 mm, 20 mm and 25 mm separation gaps. The diagrams show an exponential curve for the number of impacts on smaller values of *k*, where *k* is smaller than 200 kN/mm. The knee of the curve was in the interval between 40 and 200 kN/mm; this is true for all separation gaps. For the maximum impact force, the diagrams show a linear increase for the smaller values of k which falls between more than zero and 50 kN/mm.

Reviewing the results, it has become apparent that the *k* value have a direct effect on the number of impacts, where *k* falls between more than zero and 200 kN/mm. In addition, the maximum impact force is affected by the increase in the *k* value. It was previously proven by Anagnostopoulos (1988) that the number of impacts decreases as the separation distance between adjacent buildings increases. This fact was clearly illustrated in Fig. 11 to 14. The number of impacts range were between (130 to 730), (15 to 95), (6 to75) and (1 to 40) for 2 mm, 15 mm, 20 mm and 25 mm separation gaps, respectively. However, it was noticed that the maximum impact force is unpredicted and inconsistent with the increase in the *k* value. This is true in all separation gaps with the *k* values greater than 50 kN/mm. For instance, for the 2 mm separation gap case, when *k* was 96 kN/mm, the maximum impact force was 32 kN while when *k* was 250 kN/mm, the maximum impact force has dropped down to 26 kN and when *k* was 560 kN/mm the maximum impact force has raised up to 42 kN. This unstable linear trend maybe caused by the unpredictable nature of earthquakes. It was also noticed that the maximum impact force behaves in polynomial direction, while the number of impacts behaves in a logarithmic direction.

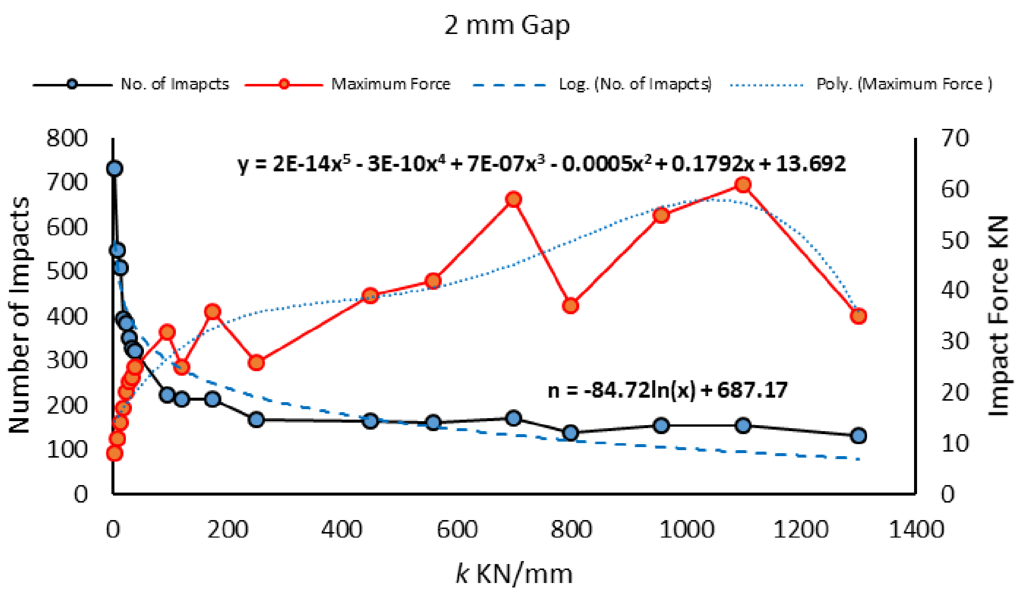

Fig. 11 Number of impacts and maximum impact force using several k values, for 2 mm gap

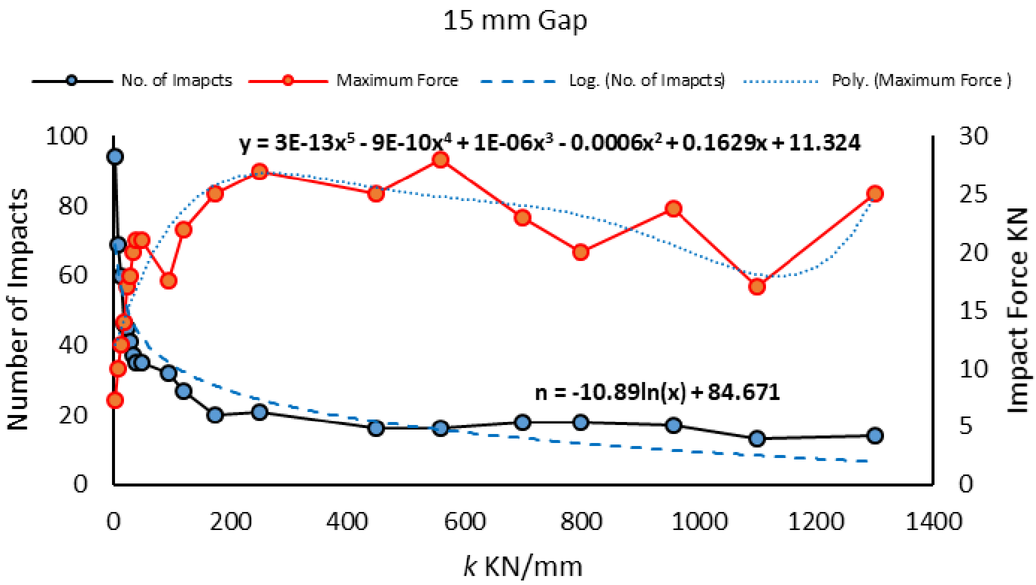

Fig. 12 Number of impacts and maximum impact force using several k values, for 15 mm gap

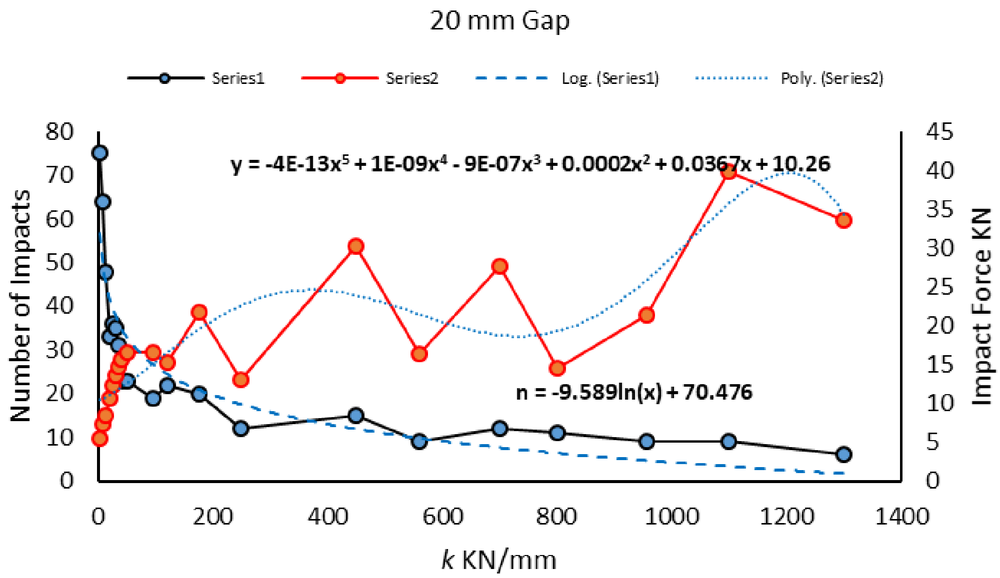

Fig. 13 Number of impacts and maximum impact force using several k values, for 20 mm gap

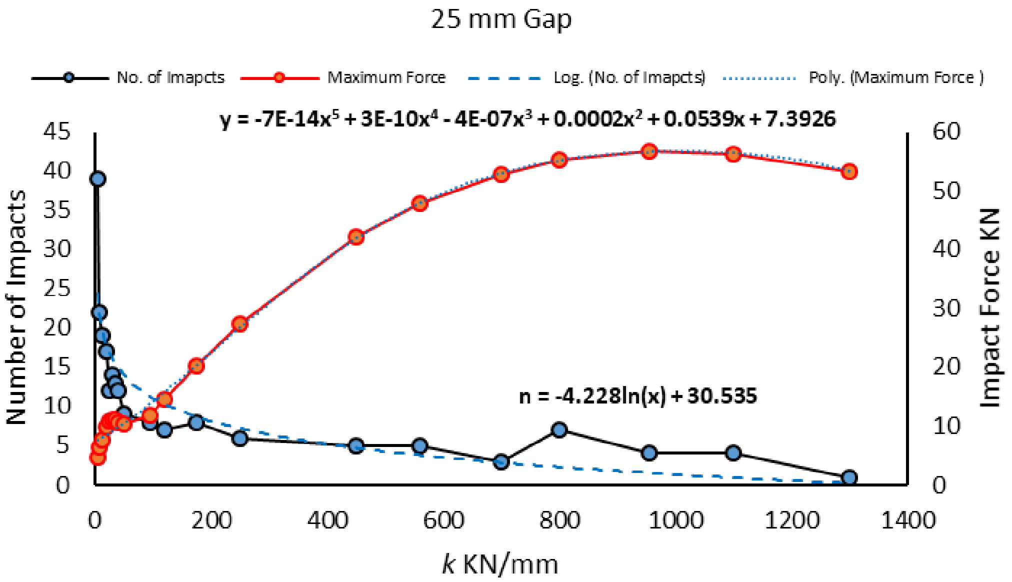

Fig. 14 Number of impacts and maximum impact force using several k values, for 25 mm gap

In order to estimate the average range of *k* values, it is recommended to involve some statistical calculations to predict the *k* value. Hence, the nonlinear regression line was plotted for the maximum impact force and the number of impacts individually as depicts in Figs. 12 to14. The aim was finding the best fit polynomial line for the maximum impact force, and the best fit logarithmic line for the number of impacts. The equations of these two regression lines can be used to calculate the average range of *k* value, where y, n and x are the maximum impact force, the number of impacts and *k* value, respectively. The polynomial equation has adapted the fifth degree order (x^5) for a better accuracy. Furthermore, the R^2 value was calculated for both lines, which shows high accuracy of the non-regression lines. The value of R^2 for all separation gaps in both lines was > 0.80. Two mathematical equations were derived for each separation gap and used to calculate the *k* value. Table 2 shows the calculation results of the four separation gaps for the number of impacts and the maximum impact force. The table shows a range of *k* values between 85 and 112 kN/mm.

Table 2 the calculated k based on the number of impacts and the maximum impact force

	2mm Gap	15mm Gap	20mm Gap	25 mm Gap
Calculated *k* based on number of impacts	112	105	103	102
Calculated *k* based on maximum impact force	90	85	105	85

The tabulated values in Table 2 were calculated as per derived equations from both lines. For each separation gap, the *k* value was calculated by using the mean and the median for the number of impacts, separately.

Similarly, the mean and the median of the maximum impact force were used to calculate the *k* value, separately. The calculated *k* value when using the mean for the number of impacts has shown a closer range, which seemed more accurate than using the median. In the median case, the *k* values were 263, 151, 174 and 207 kN/mm for 2 mm, 15 mm, 20 mm and 25 mm separation gap, respectively. However, in using the mean value case, the *k* values were 112, 105, 103 and 102 kN/mm for 2 mm, 15 mm, 20 mm and 25 mm separation gap, respectively. It's clear that the *k* values in the mean case were very close, while in the median case were much diverted. This finding was opposite to the calculation of the maximum impact force. The median of the maximum impact force has shown way closer similarity than the mean value. This concludes that the mean values may better fit the number of impacts while the median values may better fit the maximum impact force. It was found that the most appropriate range for *k* value falls between 85 and 112 kN/mm. This is true for all separation gaps, as tabulated in Table 2.

It's worth mentioning that the experimental value of *k*, which was used in Filiatrault's experiment, is far from the range found in this study. Filiatrault's value was *k* =12.8 kN/mm, while the calculated range was between 85 and 112 kN/mm, and this may be due to two main factors affecting the experiment at that time. Filiatrault performed compressive static test on each impact device to determine the element axial stiffness. Also, Filiatrault's structural models were equipped with contact points to assure the axial impact with point contact to eliminate the torsional effect of the structural model due to the uncertainty of the materials, manufacture, and installation Filiatrault et al. (1995). Moreover, the numerical simulation assumes that the colliding surfaces are ideally smooth and the pressure distribution due to the impact are uniform. However, this status is difficult to achieve in the practical engineering Guo, Cui & Li (2012).

It should be noted that the focus of this study is assisting engineers in choosing appropriate *k* values for the numerical analysis and the proposed *k* values will not be used in any experimental measurements. Instead, engineers deploy some hardware devices to detect *k* value, such as force sensor, springs and others. This is essential to understand the reasons behind the deviation that occurred between numerical and experimental values of *k*.

The median of the eight values of *k* in Table 2, was calculated in this study that is equal to (102+103)/2=102.5 kN/mm. It is close to the calculated *k* value in Equation 1.

Based on the outcomes of this study, the following equation can determine the optimal rescaled impact stiffness (*k*) value:

$$k = 102.50 \times \check{S} \times 8$$

Which can be written as:

$$k = 820 \times \check{S} \qquad (6)$$

Where $\check{S}$ denotes the scale factor used by the researchers.

The value of *k* was calculated based on 1/8 scale factor for single-bay moment resisting steel framed models. If any other scale factors is employed, then Equation 6 will be used to calculate the new *k* value. For instance, if a scale of ¼ was selected for this model; then, the equation result will be as shown below:

k= 102.5×1/4×8=205 kN/mm

Conclusions and Recommendations

The linear spring model is commonly used for describing seismic pounding between adjacent buildings with aligned slabs. In this study, an innovative approach of finding the optimum stiffness value for impact element models *k* was proposed. Initially, some parameters were abstracted from a previous experiment to reflect the real-life structural response and the experiment was numerically simulated. The *k* value range was derived from a parametric study, which proposed an optimal range of *k* values. The suggested values were tested and then evaluated by simulating them numerically. After collecting parameters from the numerical analysis, it was found that the most appropriate range of *k* values falls between 85 and 112 kN/mm. It should be noted that this is true in the models with 1/8 scale single-bay moment resisting steel frame. Researchers can rescale this range as per their own model scale factor. The proposed range *k* were found by calculating the mean value for the number of impacts and the median value for the maximum impact force. Based on the outcomes of this study, the optimal rescaled impact stiffness value can be determined from Equation 6 of this study.

Since this is essential to perform an accurate dynamic analysis in order to determine seismic pounding forces between adjacent buildings, in the absence of accurate experimental data, it is recommended that practicing engineers adopt the proposed methodology in this study in choosing appropriate *k* values for the numerical analysis.

References

Abdel Raheem, S.E. (2006), "Seismic pounding between adjacent building structures", *Electronic Journal of Structural Engineering*, **6**, 66-74, http://www.ejse.org/Archives/Fulltext/2006/200608.

Anagnostopoulos, S.A. (1988), "Pounding of buildings in series during earthquakes", *Earthquake engineering & structural dynamics*, **16** (3), 443-56, https://doi.org/10.1002/eqe.2285.

Anagnostopoulos, S.A. & Spiliopoulos, K.V. (1992), "An investigation of earthquake induced pounding between adjacent buildings", *Earthquake engineering & structural dynamics*, **21** (4), 289-302, https://doi.org/ 10.1002/eqe.4290210402.

Chau, K.T., Wei, X.X., Guo, X. & Shen, C.Y. (2003), "Experimental and theoretical simulations of seismic poundings between two adjacent structures", *Earthquake Engineering and Structural Dynamics*, **32** (4), https://doi.org/10.1002/eqe.231.

Cole, G., Dhakal, R., Carr, A. & Bull, D. (2012), "3D Modelling of Building Pounding Including Diaphragm Flexibility", *PROCEEDINGS OF THE FIFTHTEENTH WORLD CONFERENCE ON EARTHQUAKE ENGINEERING*, LISBON, PORTUGAL.

Crozet, V., Politopoulos, I., Yang, M., Martinez, J. & Erlicher, S. (2017), "Influential Structural Parameters of Pounding between Buildings during Earthquakes", *Procedia engineering*, **199**, 1092-1097, https://doi.org/10.1016/j.proeng.2017.09.084.

Far, H. (2019) 'Advanced Computation Methods for Soil Structure Interaction Analysis of Structures Resting on Soft Soils', *International Journal of Geotechnical Engineering*, **13**(4), 352-359, https://doi.org/10.1080/19386362.2017.1354510

Fatahi, B. & Tabatabaiefar, H.R. (2014) 'Effects of Soil Plasticity on Seismic Performance of Mid-Rise Building Frames Resting on Soft Soils', *Advances in Structural Engineering*, 17(10), 1387-1402, https://doi.org/10.1260/1369-4332.17.10.1387

Filiatrault, A., Wagner, P. & Cherry, S. (1995), "Analytical prediction of experimental building pounding", *Earthquake engineering & structural dynamics*, **24 (**8), 1131-54, https://doi.org/10.1002/eqe.4290240807.

Guo, A., Cui, L. & Li, H. (2012), "Impact stiffness of the contact-element models for the pounding analysis of highway bridges: experimental evaluation", *Journal of Earthquake Engineering*, vol. 16, no. 8, pp. 1132-60, https://doi.org/10.1080/13632469.2012.693243.

Huang, L.-J. & Syu, H.-J. (2014), "Free Vibration and Modal Analysis of Tower Crane Using SAP2000 and ANSYS", *Methods*, **10**, 12, http://citeseerx.ist.psu.edu/viewdoc/download?doi=10.1.1.444.5248&rep=rep1&type=pdf.

Huwaldt, J. & Steinhorst, S. (2015), "Plot Digitizer (Version 2.6. 8)[Software]".

Jankowski, R. (2005), "Non-linear viscoelastic modelling of earthquake-induced structural pounding", *Earthquake engineering & structural dynamics*, **34** (6), 595-611, https://doi.org/10.1002/eqe.434.

Jankowski, R. (2006), "Pounding force response spectrum under earthquake excitation", *Engineering Structures*, **28**, no. 8, pp. 1149-61, https://doi.org/10.1007/s40999-017-0178-7.

Jankowski, R. 2008, "Earthquake-induced pounding between equal height buildings with substantially different dynamic properties", *Engineering structures*, **30** (10), 2818-29, https://doi.org/10.1080/13632469.2012.693243.

Jankowski, R. & Mahmoud, S. (2016), "Linking of adjacent three-storey buildings for mitigation of structural pounding during earthquakes", *Bulletin of Earthquake Engineering*, **14** (11), 3075-97, https://doi.org/10.1007/s10518-016-9946-z.

Jeng, V. & Tzeng, W.L. (2000), "Assessment of seismic pounding hazard for Taipei City", *Engineering Structures*, **22** (5), 459-71, https:// Users/c3147606/Downloads/103820160707.pdf.

Kasai, K. & Maison, B.F. (1997), "Building pounding damage during the 1989 Loma Prieta earthquake", *Engineering Structures*, **19**,(3), 195-207, https://doi.org/10.1016/S0141-0296(96)00082-X.

Khatiwada, S. & Chouw, N. (2014), 'Limitations in simulation of building pounding in earthquakes', *International journal of protective structures*, **5** (2), 23-50, https://doi.org/10.1260/2041-4196.5.2.123.

Lankarani, H.M. & Nikravesh, P.E. (1992), "Hertz contact force model with permanent indentation in impact analysis of solids", *18th Annual ASME Design Automation Conference*, Publ by ASME, pp. 391-395.

López-Almansa, F. & Kharazian, A. (2018), "New formulation for estimating the damping parameter of the Kelvin-Voigt model for seismic pounding simulation", *Engineering Structures*, **175**, 284-95, https://doi.org/10.1016/j.engstruct.2018.08.024.

Mahmoud, S. & Jankowski, R. (2009), "Elastic and inelastic multi-storey buildings under earthquake excitation with the effect of pounding", *Journal of Applied Sciences*, **9** (18), 3250-62, https://doi.org/10.3923/jas.2009.3250.3262.

Mahmoud, S. & Jankowski, R. (2011), "Modified linear viscoelastic model of earthquake-induced structural pounding", *Transactions of Civil and Environemtnal Engineering*, **35**, 51-62 https://ijstc.shirazu.ac.ir/article_656_8747b85d50471766549f47134b9b4e7f.pdf.

Maison, B.F. & Kasai, K. (1992), "Dynamics of pounding when two buildings collide", *Earthquake Engineering & Structural Dynamics*, **21**(9), 771-86, https://doi.org/10.1007/s11803-015-0024-3.

Mate, N., Bakre, S. & Jaiswal, O. (2012), "Comparative study of impact simulation models for linear elastic structures in seismic pounding", *15th World Conference on Earthquake Engineering*.

Muthukumar, S. & Desroches, R. (2004), 'Evaluation of impact models for seismic pounding', *Proceedings of the 13th World Conference on Earthquake Engineering, Vancouver, Canada*.

Naderpour, H., Barros, R.C., Khatami, S.M. & Jankowski, R. (2016), "Numerical Study on Pounding between Two Adjacent Buildings under Earthquake Excitation", *Shock and Vibration*, **2016**, https://doi.org/10.1155/2016/1504783.

Naserkhaki, S., Abdul Aziz, F& Pourmohammad, H. (2012), 'Parametric study on earthquake induced pounding between adjacent buildings' *Structural Engineering and Mechanics*,**43** (4), 503-526, https://doi.org/10.12989/sem.2012.43.4.503

Newmark, N.M. (1959), "A method of computation for structural dynamics", American Society of Civil Engineers.

Noman, M., Alam, B., Fahad, M., Shahzada, K. & Kamal, M. (2016), "Effects of pounding on adjacent buildings of varying heights during earthquake in Pakistan", *Cogent Engineering*, 3(1),1225-12878, https://doi.org/10.1080/23311916.2016.1225878.

Polycarpou, P.C. & Komodromos, P. (2010), "Earthquake-induced poundings of a seismically isolated building with adjacent structures", *Engineering Structures*, **32** (7),1937-1951, https://doi.org/10.1016/j.engstruct.2010.03.011.

Rahimi, S. & Soltani, M. (2017), 'Expected extreme value of pounding force between two adjacent buildings', *Structural Engineering and Mechanics,* **61**(2) 183-192, DOI: https://doi.org/10.12989/sem.2017.61.2.183.

Rahman, A.M., Carr, A.J. & Moss, P.J. (2000), "Structural pounding of adjacent multi-storey structures considering soil flexibility effects", *12th World Conference on earthquake engineering, Article*.

SAP, C. (2000), 'Integrated software for structural analysis and design', *Analysis reference manual*.

Sheikh, M.N, Xiong, J. & Li, W.H. (2012), 'Reduction of seismic pounding effects of base-isolated RC highway bridges using MR damper', *Structural Engineering and Mechanics*, 41(6), 791-803, DOI: https://doi.org/10.12989/sem.2012.41.6.791.

Tabatabaiefar, H.R. & Clifton, T. (2016) 'Significance of Considering Soil-Structure Interaction Effects on Seismic Design of Unbraced Building Frames Resting on Soft', *Australian Geomechnics Journa*l, **51**(1), 55-64.

Tabatabaiefar, H.R., Fatahi, B. & Samali, B. (2012) 'Finite Difference Modelling of Soil-Structure Interaction for Seismic Design of Moment Resisting Building Frames', *Australian Geomechanis Journal*, **47**(3), 113-120.

Van Mier, J. & Lenos, S. (1991), 'Experimental analysis of the load-time histories of concrete to concrete impact', *Coastal engineering*, **15** (1-2), 87-106, https://doi.org/10.1016/0378-3839(91)90043-G.

Wada, A., Shinozaki, Y. & Nakamura, N. (1984), 'Collapse of building with expansion joints through collision caused by earthquake motion', *Proceedings of 8th WCEE*, **4**, 855-63.